ISSN 0023-1584, Kinetics and Catalysis, 2009, Vol. 50, No. 4, pp. 567–576. © Pleiades Publishing, Ltd., 2009.
Original Russian Text © N.M. Popova, R.Kh. Salakhova, K. Dosumov, S.A. Tungatarova, A.S. Sass, Z.T. Zheksenbaeva, L.V. Komashko, V.P. Grigor'eva, A.A. Shapovalov, 2009, published in Kinetika i Kataliz, 2009, Vol. 50, No. 4, pp. 588–598.

Nickel–Copper–Chromium Catalyst for Selective Methane Oxidation to Synthesis Gas at Short Residence Times[1]

N. M. Popova, R. Kh. Salakhova, K. Dosumov, S. A. Tungatarova, A. S. Sass, Z. T. Zheksenbaeva, L. V. Komashko, V. P. Grigor'eva, and A. A. Shapovalov

Sokol'skii Institute of Organic Catalysis and Electrochemistry, Almaty, Kazakhstan

e-mail: tungatarova58@mail.ru; orgcat@nursat.kz

Received July 3, 2006; in final form, July 16, 2008

Abstract—Data on the selective oxidation of methane to synthesis gas on a 9% NiCuCr/2% Ce/$(\theta + \alpha)$-Al_2O_3 catalyst in dilute mixtures with Ar at short residence times (2–3 ms) are presented. The composition, structure, morphology, and adsorption properties of the catalyst with respect to oxygen and hydrogen before and after reaction were studied using XRD, BET, electron microscopy with electron microdiffraction, TPR, TPO, and TPD of oxygen and hydrogen. The following optimum conditions for the preparation and pretreatment of the catalyst for selective methane reduction were found: the incipient wetness impregnation of a support with aqueous nitrate solutions; drying; and heating in air at 873 and then at 1173 K (for 1 h at either temperature) followed by reduction with an H_2–Ar mixture at 1173 K for 1 h. At a residence time of 2–3 ms (space velocity to 1.5×10^6 h^{-1}) and 1073–1173 K, the resulting catalyst afforded an 80–100% CH_4 conversion in mixtures with O_2 ($CH_4/O_2 = 2 : 1$) diluted with argon (97.2–98.0%) to synthesis gas with $H_2/CO = 2 : 1$. The selectivity of CO and H_2 formation was 99.6–100 and 99–100%, respectively; CO_2 was almost absent from the reaction products. The catalyst activity did not decrease for 56 h; carbon deposition was not observed. A possible mechanism of the direct oxidation of CH_4 to synthesis gas is considered.

DOI: 10.1134/S0023158409040144

INTRODUCTION

Methane and its homologs are permanent components of natural gas and petroleum; they are released in coal mining, etc. Because of this, the activation and involvement of these compounds in new chemical reactions can become an inexhaustible source of various hydrocarbon materials and organic synthesis intermediates and products.

Commercial steam reforming of natural gas to produce CO and H_2 for the subsequent synthesis of methanol is currently the main process for the chemical conversion of CH_4. Large energy consumption and a high H_2/CO ratio in the resulting mixture are the advantages of this process. The chlorination of CH_4 to CCl_4, the oxidative interaction of methane with NH_3 to form HCN, CH_4 electrocracking to form a mixture of acetylene with ethylene, flame pyrolysis to produce a mixture of acetylene with CO and H_2, and the synthesis of gasoline and other liquid fuels from ethane–ethylene fractions obtained by the thermal pyrolysis and dehydrogenation of ethane on zeolite catalysts have also been commercialized [1, 2].

In the past decade, a new process for the production of synthesis gas by the direct oxidation of CH_4 in an oxygen deficiency at a short residence time has been actively developed. Prettre et al. [3] were the first to perform this reaction on a Ni catalyst in 1946. In the 1990s, this reaction has been studied with the use of a reactor with porous block catalysts (a millisecond reactor) [2, 4–7]. It was found that synthesis gas was formed with high selectivity (the selectivity of H_2 and CO formation was ~80%) from a mixture with $CH_4/O_2 > 2 : 1$ on reduced supported Pt, Pd, and Rh catalysts at residence time $\tau = 10^{-2}$–10^{-4} s and a high temperature [4–6]. The best results were obtained with the use of a Rh catalyst on Al_2O_3 [8].

The use of block catalysts makes it possible to considerably decrease the reactor volume as compared with that of reactors used in CH_4 steam reforming [9] and to develop an alternative process for the production of synthesis gas, which is suitable for the manufacture of methanol and for other purposes.

A thermodynamic analysis indicated that the preliminary incomplete combustion of CH_4 with the formation of a mixture of CO + H_2 at an elevated pressure considerably decreases energy consumption in a gas turbine cycle in terms of 1 mol of consumed methane [10].

More recently, noble metals (Rh, Ru, Pd, Pt, and Ir) on various supports; Ni, Co, and Fe oxides; and perovskites have been widely used in the selective oxidation of methane to synthesis gas. An analysis of published data showed that, at a ratio of $CH_4/O_2 \geq 2 : 1$, this reaction can occur on reduced catalysts over the

[1] Reported at the VII Russian Conference on Mechanisms of Catalytic Reactions (with international participation), St. Petersburg, July 2–8, 2006.

temperature range of 1023–1173 K at high space velocities (to 1×10^5 h^{-1}). In this case, the CH_4 conversion into a mixture of $H_2/CO = 2 : 1$ was 80–100% and the selectivity of H_2 and CO formation was also as high as 80–100%. The process of selective methane oxidation stably occurred on Rh/α-Al_2O_3, Rh/ceramics [4–6, 11], Pt–Rh–Pd on ceramics [12], and Rh/$ZrO_2 \cdot CeO_2$/α-Al_2O_3 [13] catalysts and Ni perovskites promoted with Pt, Rh, and Ru [14–20] for 100–700 h at space velocities V to 10×10^5 h^{-1} ($\tau = 10^{-2}$–10^{-4} s). The Ni/MgO catalysts [21]; Ni–La and Li–Ni–La perovskites on $MgAl_2O_4$ [22] and Al_2O_3 [23, 24]; Ni–Co on Mg, Ce, and Zr [25]; $BaTi_{0.8}Ni_{0.2}O_3$ [26] and $Ba_{0.5}Sr_{0.5}Co_{0.8}Fe_{0.2}O_3$ perovskites [27, 28] ($V = 2 \times 10^3$–7×10^4 h^{-1}); and molybdenum carbides ($V = 5.2 \times 10^3$ h^{-1}) [29] were characterized by lower outputs. Mixed Ni–Fe [30], Ni–Ce [31], and Ni–Co catalysts [25] ($V = (0.9–1.5) \times 10^5$ h^{-1}) exhibited high outputs. The addition of a second transition element to nickel increases the dispersity of Ni particles; facilitates the reduction of Ni; decreases the temperature of selective methane oxidation; and, in a number of cases (Ni–Rh, Ni–Cu, and Ni–Fe), facilitates the formation of bimetallic clusters. It is likely that the reacting components are independently adsorbed and activated on the mixed catalysts: CH_4 on Ni and O_2 on the second element or an oxide support (CeO_2 or La_2O_3). Data on the use of mixed Ni catalysts in the reaction of selective methane oxidation [25, 31] indicate that further studies are required in order to abandon the use of noble metals.

In this work, we examined a mixed Ni–Cu catalyst. According to published data, the (8.0% Ni + 1.0% Cu)/SiO_2 catalyst decomposed CH_4 into H_2 and carbon, which was readily oxidized with carbon dioxide for 120 h with the use of a mixture of $CH_4 + CO_2$, in an inert atmosphere at 1033 K [32]. Janlai et al. [33] used the (1.8% Ni + 0.8% Cu)/Al_2O_3 catalyst for CH_4 transformation under the action of CO and H_2O; however, the degree of reactant conversion was low. In the absence of oxygen, the Ni–Cu catalyst (from 8 to 50% Cu) on Al_2O_3 stably decomposed CH_4 into H_2 and soot [34, 35]. At the Boreskov Institute of Catalysis, Siberian Branch, Russian Academy of Sciences (Novosibirsk), a wasteless technology was developed for the production of a Ni–Cu catalyst (for the decomposition of CH_4) by the mechanochemical activation of copper and nickel oxides together with aluminum and magnesium hydroxides (69–74% NiO and 9.5–12% CuO) followed by reduction [36–38].

The use of Ni–Cu catalysts in redox processes is based on the ability of Ni and Cu to form substitutional solid solutions with a face-centered cubic lattice at Cu concentrations to 60–80 vol %. For example, the highest catalyst activity and selectivity in fat hydrogenation was reached when the surface concentration of copper was higher than the concentration of nickel by a factor of 2–3 [39, 40]. The previously developed Ni–Cu catalyst (atomic ratio of Ni/Cu = 1 : 3) with a chromium additive was used for the hydrogenation of fats [41, 42] and for the deep oxidation of CO, CH_4, and other organic compounds in processes for the removal of harmful impurities from waste gases at furniture factories (Almaty and Tashkent) and in the manufacture of cables (Samara) and streptomycin (Kiev) [43, 44].

We studied the effects of the ratio between the supported elements, the concentrations of these elements on the support surface, and the order of supporting upon the properties of the resulting catalyst. At a 7–10% total concentration of the supported elements, metal oxide clusters were formed on the surface and alumina granules were fully and uniformly impregnated. The atomic ratio Ni/Cu/Cr = 1 : 3 : 0.1 was optimal in both fat hydrogenation and CO oxidation [42, 43].

The Ni–Cu–Cr catalysts on Al_2O_3, Keles clay, and activated carbon are highly pyrophoric; as found by dehydrogenation with *para*-benzoquinone, they can sorb a considerable amount of hydrogen [45]. Under anodic polarization with *para*-benzoquinone, the major portion of hydrogen was desorbed at high anodic potentials; this fact suggests that hydrogen was tightly bound to the catalyst [46].

Thus, the currently available data on the properties of Ni–Cu–Cr catalysts suggest that these catalysts in a reduced state can activate and decompose CH_4 and sorb the resulting hydrogen in the bulk after decomposition. In this work, we used the 9% NiCuCr/(θ + α)-Al_2O_3 catalyst modified with 2% Ce.

EXPERIMENTAL

The Ni–Cu–Cr catalyst was prepared by the incipient wetness impregnation of the cerium-modified microspherical granules of (θ + α)-Al_2O_3 (granule size, 100–200 μm; specific surface area, $S_{sp} = 57.7$ m^2/g) with aqueous solutions of corresponding metal nitrates [47]. The metal contents of the catalyst were as follows (wt %): Ni, 2; Cu, 6.7; Cr, 0.2; and Ce, 1.8. The total concentration of Ni, Cu, and Cr was about 9%.

As found by derivatography, the catalysts were formed in two steps: initially, the starting components interacted with the surface of Al_2O_3 to form hydrated complex compounds; thereafter, the dehydration and decomposition of metal nitrates occurred. Physisorbed water was removed at 350–370 K; dehydration occurred at 440–460 K (endotherm); transition metal nitrates decomposed at 560–620 K (exotherm), and cerium nitrate decomposed with the formation of an oxide at 780–875 K. Based on these data, we used the following conditions for the thermal treatment of the catalysts: drying at 450–470 K for 4–5 h; heating at 873 K for 1–1.5 h; calcination in air under conditions of slowly increasing temperature to 1173 K; and, finally, reduction with a mixture of $H_2/Ar = 40 : 60$ (by volume) at 1173 h for 1 h.

The selective catalytic oxidation of methane, which was present in a low concentration in a mixture of $CH_4/O_2/Ar$ = (1.4–2.2) : (0.6–0.8) : (97–98) (by volume), was performed in a flow reactor (inner diameter of 4.5 mm) on a 9% Ni–Cu–Cr catalyst (a sample of 10 mg) in accordance with a published procedure [16]. To perform the reaction under conditions close to a plug-flow mode and to produce isothermal conditions, catalyst grains were mixed with an inert material (quartz, particle size of 0.20–0.25 mm) in a ratio of 1 : 43.

The compositions of gas mixtures at the reactor inlet and outlet (the experiment time was 180 min) were determined on an LKhM-72 chromatograph with a thermal conductivity detector. A column packed with NaX was used in the analysis for H_2, O_2, N_2, CH_4, and CO, and a column with Polysorb 2 was used for the determination of CO_2.

The phase composition of the catalysts was determined on a DRON-4-7 X-ray diffractometer with a Co anode (25 kV; 25 mA; 2θ = 15°–80°). The morphology, size, and chemical composition of particles were studied using an EM-125 K transmission electron microscope at a magnification of up to 100000 with the use of a replica technique and electron microdiffraction. A multipurpose vacuum system was used for the sputtering of carbon replicas; the catalyst support was dissolved in HF. The microdiffraction patterns were identified using JSPDS data (1986). The specific surface areas of the catalysts were determined by the BET method on an Accusorb instrument (Micromeritics, United States) using the low-temperature adsorption of N_2. The temperature-programmed desorption (TPD) of oxygen and temperature-programmed reduction (TPR), which were described in greater detail elsewhere [48], were used for measuring the amounts of oxygen sorbed by catalysts and for characterizing this oxygen and its ability to react with a reducing agent (H_2).

Before the TPD of oxygen, the traces of H_2O, OH groups, and CO_2 were removed from catalysts, which were preheated at 873 K in air, by vacuum training at 573 K and 10^{-5} Torr for 1 h. Then, the sample was treated with oxygen at 673 K (treatment time, 1 h; flow rate, 40 ml/min). The ability of the reduced catalysts to absorb oxygen from its mixture with He (10% O_2) was evaluated by gradually increasing temperature under programmed conditions at a rate of 8 K/min with the use of a thermal conductivity detector.

The activation energies of desorption of O_2 and H_2 were determined using a modified Polanyi–Wigner equation from the temperature dependences of their concentrations [49]. The TPD of hydrogen from the 9% NiCuCr/2% Ce/(θ + α)-Al_2O_3 catalyst, which was preevacuated for 0.5 h and reduced, was performed by increasing temperature at a linear rate of 15 K/min from 393 K to a stabilization temperature (1173 K) in a flow of argon (60 ml/min) on a Setaram adsorption system (France) equipped with a thermal conductivity detector.

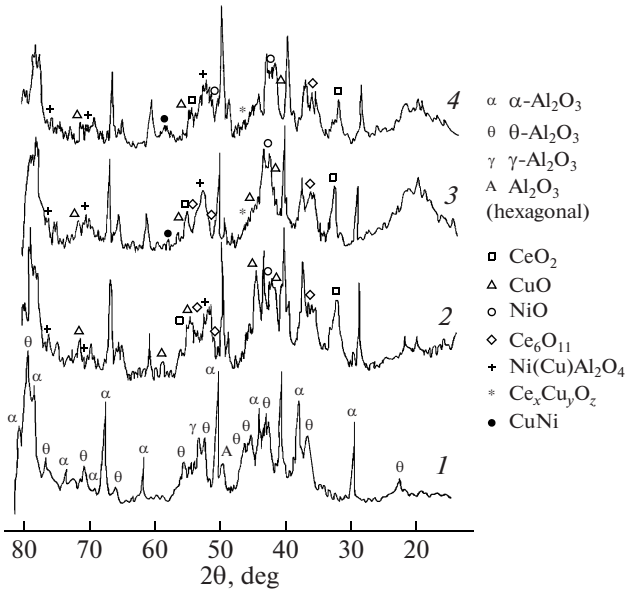

Fig. 1. X-ray diffraction patterns of (*1*) the support and the 9% NiCuCr/2% Ce/(θ + α)-Al_2O_3 catalyst after heating in air at (*2*) 873 or (*3*) 1173 K and (*4*) after reduction at 1173 K.

RESULTS AND DISCUSSION

X-ray Diffraction Analysis and Electron Microscopy with Electron Microdiffraction

An XRD study [50] demonstrated that the initial Ni–Cu–Cr catalyst after heating at 873 K (Fig. 1, spectrum *2*) contained θ- and α-Al_2O_3; the nanoparticles (20–100 Å) of Ni (reflections with d/n = 2.4 and 2.08 Å) and Cu oxides (2.52, 2.33, 1.91, 1.79, and 1.51 Å) or their mixtures; CeO_2 (intense reflections at 3.13 and 1.91 Å); Ce_6O_{11} (2.80 and 1.96 Å); $Ni(Cu)Al_2O_4$ aluminates (low-intensity reflections at 2.44, 1.99, 1.53, and 1.42 Å); and other phases (200 Å), which can be ascribed to $CuCrO_2$ (1.63 and 1.54 Å), $NiCrO_4$, and Cr_5O_{12}.

Further heating caused considerable changes in the phase composition of the catalyst: the crystallization of CeO_2 and the transformation θ-Al_2O_3 ⟶ α-Al_2O_3 occurred (Fig. 2). Above 1073 K, the concentration and particle size of $Ni(Cu)Al_2O_4$ increased. As a result of these processes, the total specific surface area decreased from 60 to 5–8 m^2/g.

As can be seen in Fig. 1 (spectrum *3*), the intensity of reflections due to CuO and NiO considerably decreased after heating at 1173 K. A wide region of intense absorption (halo) appeared at 2θ = 15°–30°; this suggests an increase in the concentration of X-ray amorphous oxide phases.

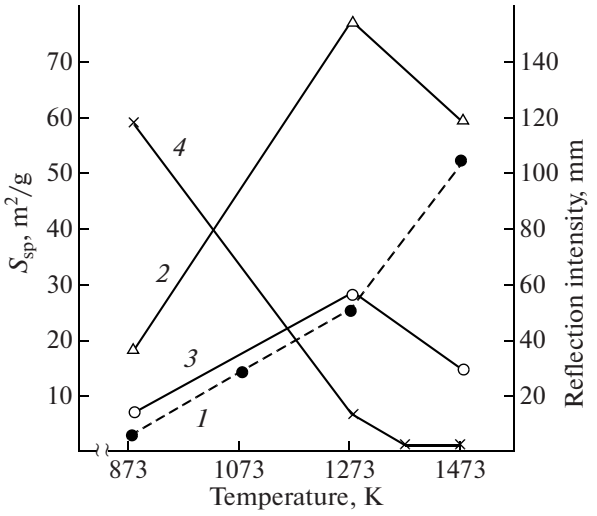

Fig. 2. Effect of the temperature of heating in air (for 5 h at each temperature point) of the 9% NiCuCr/2% Ce/(θ + α)-Al_2O_3 catalyst on (*4*) its specific surface area and reflection intensities: (*1*) Ni(Cu)Al_2O_4(1.43 Å), (*2*) α-Al_2O_3 (1.74 Å), and (*3*) CeO_2 (1.91 Å).

After reduction with hydrogen at 1173 K, the concentration of aluminates in the catalyst decreased (Fig. 1, spectrum *4*) and the particles of Ni ($d/n = 2.06$ and 1.67 Å), Cu (2.08 and 1.81 Å), Ce_6O_{11} (50–60 Å), CeO_2 and mixed phases $Ce_xCu_yO_z$ (2.24 and 2.72 Å) appeared (see Fig. 3c).

Electron-microscopic analysis with electron microdiffraction demonstrated that the initial Ni–Cu–Cr catalyst (Fig. 3a) contained NiO and CuO particles (30–50 Å) and Cu (30–50 Å) and Ni (to 100 Å) aluminates. Heating at a higher temperature (1473 K, Fig. 3b) caused an increase in the particle size of aluminates to 200 Å or more.

The electron micrographs of the catalyst reduced at 1173 K (Fig. 3c) exhibit semitransparent films and disperse dense fine particles of size ~40 Å [51]. The corresponding microdiffraction pattern has a shape of wide rings, which correspond to Cu^0 and Ni^0 metals. The composition of the compound is described by the formula $NiCu_{3.8}$. The Cu^0 and Ni^0 metals are also the constituents of films with consolidations. Ce_6O_{11} is shown as semitransparent particles (50–60 Å) in the micrographs.

The catalyst after 56-h-long operation under conditions of selective methane oxidation without a decrease in the activity consisted of Ce_6O_{11}, Cu^0, and Ni^0 particles (50–100 Å) and the $NiCu_{3.8}$ compound as a polycrystalline film and coarser dense aggregates of disperse particles of size 50 Å (Fig. 3d). The formation of carbon particles on the catalyst was not observed.

Thus, the XRD and electron microscopic studies with electron microdiffraction demonstrated that the initial 9% NiCuCr/2% Ce/(θ + α)-Al_2O_3 catalyst was a mixture of Cu^0 and Ni^0 metals, $NiCu_{3.8}$ as a polycrystalline film, and Ce_6O_{11} oxides (of size 50–60 Å) on the surface of α-Al_2O_3.

Temperature-Programmed Reduction, Oxidation, and Desorption Studies

The use of TPR and the TPD of oxygen from Ni–Cu–Cr catalysts supported on 2% Ce/(θ + α)-Al_2O_3 made it possible to study in more detail the mechanisms of reduction and oxygen release from oxides and to evaluate the ability of the catalysts to adsorb O_2 from a gas phase [52].

Figure 4 shows the TPR spectra of the 9% NiCuCr/2% Ce/(θ + α)-Al_2O_3 catalyst heated at (*1*) 873, (*2*) 973, (*3*) 1173, and (*4*) 1473 K in air and (*5*) sample *4* reduced at 1223 K and reoxidized at 973 K, as well as the TPO spectra of catalysts *1*, *3*, and *4*. In Fig. 4, it can be seen that the TPR spectrum of the catalyst heated at 873 K exhibited four peaks of H_2 consumption. According to published data [35, 53, 54], these peaks correspond to the reduction of CuO (maximum temperature $T_{max} = 523$ K), NiO–CuO mixed oxides ($T_{max} = 573$ K), NiO ($T_{max} = 673$ K), CeO_2, and, partially, the resulting aluminates of Ni and Cu ($T_{max} = 1073$ K). As the heating temperature was increased, the intensity of these peaks decreased. After heating at 1473 K, peaks corresponding to the reduction of NiO, CuO, and mixed oxides disappeared and the absorbed hydrogen was consumed for the reduction of CeO_2 and the reductive decomposition of Ni and Cu aluminates (spectrum *4*).

In the course of TPO, the adsorption of oxygen initially occurred ($T_{max} = 523$ K) and then metal oxides were formed ($T_{max} = 673$ and 800 K). The catalyst heated at 1473 K, which contained Ni and Cu aluminates (spectrum *4*), was also capable of sorbing O_2 at low temperatures (spectrum *4'*) after the reductive decomposition of the aluminates at temperatures to 1223 K. This suggests that the reduction of the heated catalyst at 1173–1223 K facilitated the appearance of Cu^0 and Ni^0 on the surface; oxides were formed upon the reduction of these metals, and the reduction of these oxides under TPR conditions manifested itself as a single peak at 1173 K (spectrum *5*).

Thus, although catalyst elements deeply interacted with the support in the course of oxidative treatment and this interaction was accompanied by the formation of Ni and Cu aluminates, the subsequent treatment with hydrogen at 1173–1223 K resulted in the complete decomposition of these aluminates and the formation of Ni^0 and Cu^0 metals, which readily interact with oxygen, on the surface.

Thermal Desorption of Oxygen

In a previous study of the 9% NiCuCr/(γ + θ)-Al_2O_3 catalyst heated in an atmosphere of O_2 at 873 K, it was found [55] that the TPD curve of oxygen preadsorbed at 673 K exhibited inflections at 773 and 923 K and a

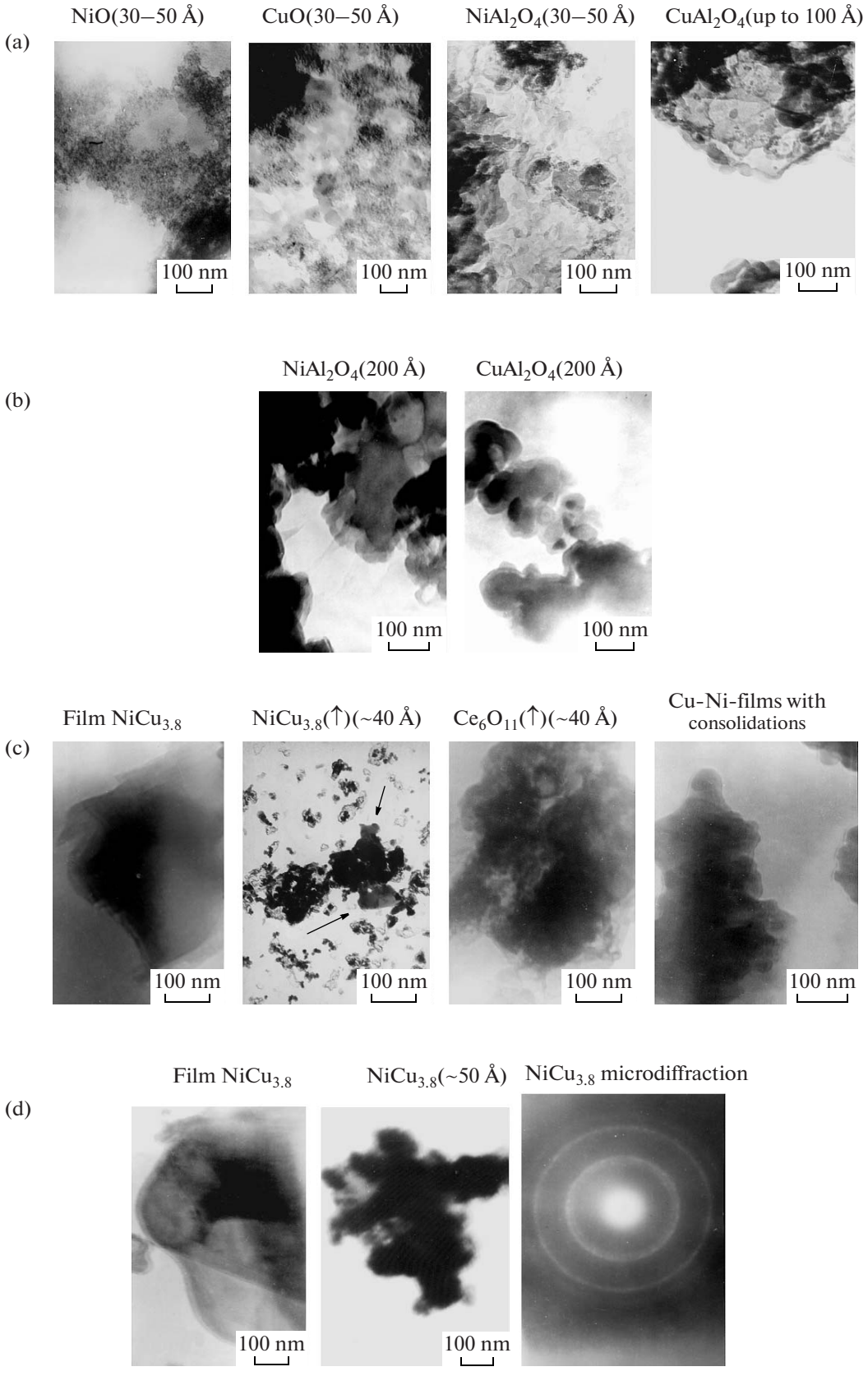

Fig. 3. Electron micrographs of 9% NiCuCr/2% Ce/(θ + α)-Al_2O_3 catalyst samples: (a) after heating at 873 K, (b) after heating at 1473 K, (c) after reduction with hydrogen at 1173 K, and (d) after the selective oxidation of CH_4 at 1173 K for 56 h.

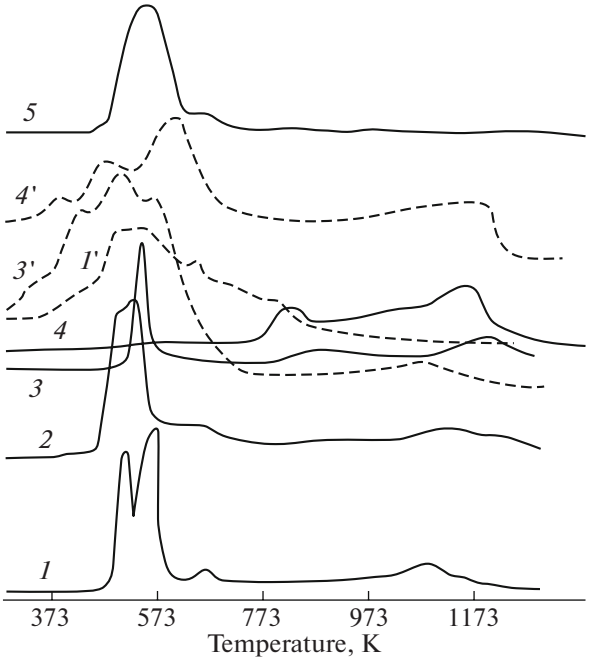

Fig. 4. TPR spectra (solid lines) of 9% NiCuCr/2% Ce/(θ + α)-Al_2O_3 samples heated in air at (*1*) 873, (*2*) 973, (*3*) 1173, and (*4*) 1473 K and (*1'*, *3'*, and *4'*) the TPO spectra (dashed lines) of samples *1*, *3*, and *4*, respectively, reduced at 1175–1225 K. (*5*) The TPR spectrum of the catalyst initially reduced at 1223 K and then reoxidized at 973 K.

maximum at 1023–1270 K. They appeared because of the desorption of adsorbed oxygen (in the range of 670–870 K) and the decomposition of copper oxide, mixed oxides, and, partially, Ni and Cu aluminates (above 1173 K). The activation energy of oxygen desorption is 88.0 ± 8.8 kJ/mol, and the activation energy of O_2 release from mixed oxides is 144.0 ± 14.4 kJ/mol.

This pattern is also consistent with the TPD spectrum of oxygen from the 9% NiCuCr/2% Ce/(θ + α)-Al_2O_3 catalyst (Fig. 5, curve *1*). In this case, the activation energy of oxygen desorption is 90.8 kJ/mol, and the activation energy of decomposition of mixed oxides is 142.0 ± 14.2 kJ/mol.

After a long-term heating of the catalyst at 1473 K, the first peak (desorption of adsorbed oxygen) fully disappeared from the TPD spectrum and the release of oxygen dramatically decreased in the region of decomposition of Ni and Cu oxides and at a stabilization temperature of 1070 K (spectrum *2*). This can be explained by the fact that the major portion of metal oxides reacted with the support to form Ni(Cu)Al_2O_4 aluminates, as found by XRD analysis and electron microscopy. After the reduction of the catalyst with hydrogen at 1273 K and the adsorption of O_2 on it, the TPD spectrum of oxygen approached its initial shape (Fig. 5, spectrum *3*). The catalyst became capable to adsorb oxygen once again (desorption temperature of

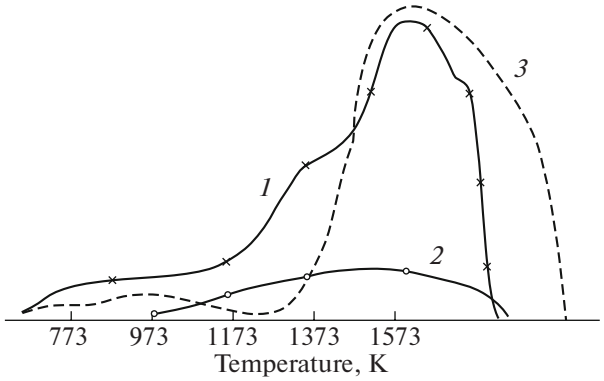

Fig. 5. Thermal desorption of oxygen from the 9% NiCuCr/2% Ce/(θ + α)-Al_2O_3 catalyst: (*1*) after heating at 873 K in air, (*2*) after heating at 1473 K in air, and (*3*) after reduction with an H_2–Ar mixture at 1273 K.

673–873 K) and to form Ni and Cu oxides (desorption temperature above 973 K).

These results are fully consistent with those obtained by XRD analysis, TPR, and TPO in a study of the redox treatment of the Ni–Cu–Cr catalyst.

Thermal Desorption of Hydrogen

Figure 6 shows the TPD spectra of hydrogen from the 9% NiCuCr/2%Ce/(θ + α)-Al_2O_3 catalyst, which was heated at 1173 K and reduced at various temperatures, over a range from 293 to 1373 K (stabilization temperature). Desorption occurred in two regions: narrow (373–733 K; T_{max} = 443–483 K), which corresponds to the molecular adsorption of hydrogen, and wider (773–1373 K; T_{max} = 1060–1141 K), which

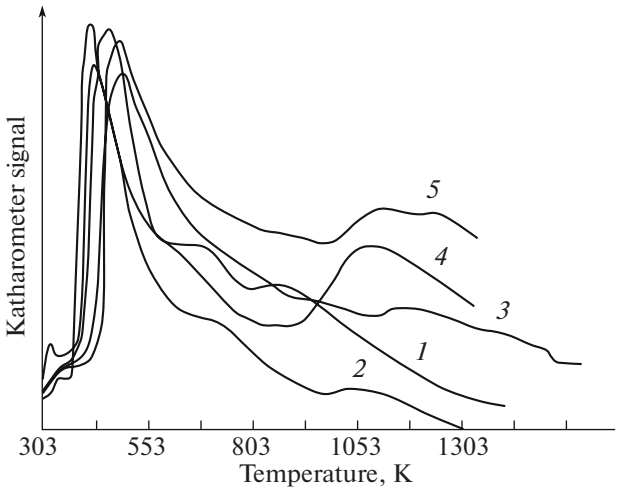

Fig. 6. Thermal desorption of hydrogen from the 9% NiCuCr/2% Ce/(θ + α)-Al_2O_3 catalyst heated at 1173 K in air and reduced with an H_2–Ar mixture at (*1*) 673, (*2*) 873, (*3*) 973, (*4*) 1073, and (*5*) 1173 K.

Table 1. Effect of the temperature of hydrogen adsorption on the parameters of hydrogen desorption from the 9% NiCuCr/2% Ce/(θ + α)-Al_2O_3 catalyst (sample of 0.25 g)

Reduction temperature, K	Time, h	Total amount of desorbed hydrogen, 10^{-5} mol/g_{Cat}	Region I		Region II	
			amount of desorbed hydrogen, 10^{-5} mol/g_{Cat}	H/Ni	amount of dissolved hydrogen, 10^{-5} mol/g_{Cat}	H/Ni
673	3	13.44	7.14	1.60	Not determined	–
873	3	13.98	7.14	1.60	0.35	0.085
973	3	15.07	7.85	1.88	1.42	0.34
1073	1	16.25	6.78	1.60	4.64	1.11
1173	1	21.50	7.85	1.88	8.57	2.03

Table 2. Effect of space velocity (residence time) on the selective catalytic oxidation of CH_4 to CO and H_2 on the 9% NiCuCr/2% Ce/(θ + α)-Al_2O_3 catalyst reduced at 1173 K

$V \times 10^5$, h^{-1}	τ, ms	Outlet concentration, %			x_{CH_4}, %	Selectivity, %			H_2/CO
		CO	CO_2	H_2		CO	H_2	CO_2	
18.0	2.00	1.20	0	2.40	77.42	100	100	0	2.00
16.2	2.22	1.25	0	2.50	80.65	100	100	0	2.00
15.3	2.35	1.40	0	2.80	87.50	100	100	0	2.00
14.4	2.49	1.40	0	2.79	96.55	100	99.64	0	1.99
13.5	2.67	1.385	0.005	2.77	99.29	99.64	99.64	0.36	2.00
12.6	2.86	1.445	0.005	2.89	100	99.66	99.66	0.34	2.00
11.7	3.27	1.395	0.005	2.79	100	99.64	99.64	0.36	2.00
10.8	3.33	1.37	0.03	2.77	100	97.86	98.93	2.14	2.02
10.2	3.50	1.46	0.04	2.93	100	97.33	97.67	2.67	2.01
9.9	3.64	1.36	0.04	2.80	100	97.14	100	2.86	2.06
9.0	4.00	1.38	0.02	2.80	100	98.57	100	1.43	2.03
7.2	5.00	1.44	0.01	2.90	100	100	100	0.69	2.01
4.5	8.00	1.495	0.005	3.00	100	100	100	0.33	2.01

Note: Reaction temperature, 1173 K; $CH_4/O_2 = (1.9–2.0) : 1$; the tabulated values were obtained 1 h after the start of the reaction.

corresponds to the desorption of H_{ads} and hydrogen dissolved in the catalyst structure (above 700 K). In the latter region, peaks appeared only in the case that the catalyst was reduced at a temperature of no lower than 1073 K.

In Table 1, it can be seen that the total amount of desorbed hydrogen increased from 13.4×10^{-5} to 21.5×10^{-5} mol/g_{Cat} as the reduction temperature was increased from 673–873 to 1173 K. In this case, it varied from 6.8 to 7.9×10^{-5} mol/g_{Cat} in the former region and reached a maximum value of 8.6×10^{-5} mol/g_{Cat} in the latter region (the most strongly bound hydrogen).

Data obtained using TPR and electron microdiffraction indicate that, at temperatures higher than 1000 K, Ni and Cu oxides began to reduce to metals and then formed a $NiCu_{3.8}$ alloy, and molecular hydrogen, which desorbed in the former region, can be adsorbed on their surface.

The appearance of the most strongly bound hydrogen, which desorbed above 873 K, was due to its dissolution in the lattice of Ni^0 and the alloy of nickel with copper (the ratio between hydrogen and the metal varied from 1.10 to 2.03). The alloy was formed only after the reduction of the catalyst at high temperatures. Published data [56, 57] are indicative of the dissolution of hydrogen at temperatures higher than 1200 K with the incorporation of hydrogen into octahedral interstitial voids of the lattice of Ni^0 and its alloys. Previously, in a study of the Ni–Cu–Cr catalyst on active carbon containing 33% Ni, it was also found that a portion of hydrogen was desorbed very slowly [45]. An analysis of the charging curves of the 12% NiCuCr/clay catalyst in anodic polarization with *para*-benzoquinone demonstrated the presence of strongly bound hydrogen, as distinct from a monometallic Ni catalyst [46].

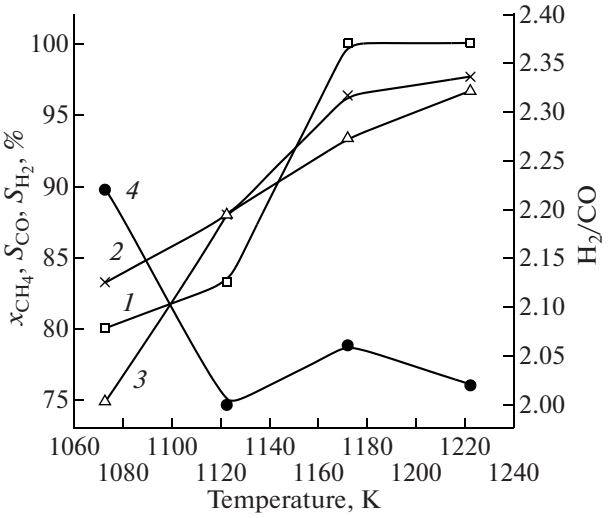

Fig. 7. Effect of temperature on (*1*) the conversion of methane, the selectivity of (*2*) H_2 and (*3*) CO formation, and (*4*) the H_2/CO ratio in the reaction of selective methane oxidation on the 9% NiCuCr/2% Ce/(θ + α)-Al_2O_3 catalyst. $CH_4/O_2 = 1.9 : 1$; $\tau = 3.5$ ms; $V = 1.02 \times 10^6$ h^{-1}.

Thus, the TPD of hydrogen demonstrated that the Ni–Cu–Cr catalyst can sorb hydrogen not only on the surface (H_{2ads}); its structure also contained strongly bound, dissolved hydrogen.

Catalytic Activity

The selective methane oxidation reaction was performed on the 9% NiCuCr/2% Ce/(θ + α)-Al_2O_3 catalyst, which was heated at 1173 K in air and then reduced with an H_2–Ar mixture (40 : 60, by volume) at 1173 K. The effects of temperature, CH_4/O_2 ratio, and residence time on the process were studied.

Table 2 shows the effect of residence time (τ from 2 to 8 ms) on the selective oxidation of methane (CH_4 concentration of 1.40–1.45%) with a mixture of O_2 with Ar (0.7–0.8% O_2) at a CH_4/O_2 ratio of 1.9 : 1. The degree of oxygen conversion (x_{O_2}) was 100% at all residence times, and the complete conversion of CH_4 was reached starting at $\tau = 2.67$ s. The H_2 /CO concentration ratio at the reactor outlet was 2 : 1 at any τ. For the most part, the selectivity of CO formation (S_{CO}) was 99–100%, and it decreased to 97% only at $\tau = 3.30$–3.64 s because of the formation of a comparatively small amount of CO_2. The balance on carbon over starting and resulting products was 100%.

Table 3. Effect of the CH_4/O_2 ratio on the main characteristics of the reaction of selective methane oxidation at 1173 K on the 9% NiCuCr/2% Ce/(θ + α)-Al_2O_3 catalyst reduced at 1173 K

$CH_4 : O_2$	x_{CH_4}, %	x_{O_2}, %	S_{CO}, %	S_{H_2}, %	H_2/CO
2.0 : 1	80.65	100	100	100	2.00
2.6 : 1	63.89	100	99.13	91.30	1.84
2.8 : 1	58.97	100	99.13	89.56	1.81
3.75 : 1	51.11	100	100	82.61	1.65

Note: The tabulated values were obtained 1 h after the onset of reaction; $\tau = 2$–2.4 ms.

Figure 7 shows data on the effect of reaction temperature on the conversion of CH_4 and the selectivity of formation of selective methane oxidation products. In the range from 1073 to 1223 K ($CH_4/O_2 = 1.9 : 1$; $\tau = 3.5$ ms; space velocity, 1.02×10^6 h^{-1}), the conversion of methane (x_{CH_4}) increased from 80 to 100% and the selectivity of H_2 and CO formation increased from 75 to 94–96%.

Table 3 illustrates the effect of the $CH_4 : O_2$ ratio in the starting reaction mixture on x_{CH_4}, S_{CO}, and S_{H_2} at similar values of τ (2–2.4 ms) and a temperature of 1173 K. As CH_4/O_2 was increased from 2 : 1 to 3.75 : 1, x_{CH_4} decreased from 81 to 51%, S_{CO} remained unchanged and close to 100%, and S_{H_2} decreased from 100 to 83%. At the ratio $CH_4/O_2 = 2 : 1$, a maximum value of $x_{CH_4} = 80.6\%$ was reached at S_{CO} and $S_{H_2} = 100\%$ and an optimum value of $H_2/CO = 2 : 1$.

The above data suggest that the reduced Ni–Cu–Cr catalyst supported on alumina promoted with cerium can selectively perform the complete oxidation of methane at 1173 K to synthesis gas with $H_2/CO = 2$ at very short residence times (2.8–8.0 ms).

CONCLUSIONS

Thus, in this work, we used a number of physicochemical techniques to optimize conditions for the preparation and pretreatment of the 9% NiCuCr/2% Ce/(θ + α)-Al_2O_3 catalyst for the selective oxidation of methane to synthesis gas. These conditions include the impregnation of the modified support with aqueous solutions of metal nitrate salts and drying followed by heating in air at 873 K and then at 1173 K for 1 h at either temperature and reduction with an H_2–Ar mixture for 1 h at 1173 K. Initially, the nanoparticles of Ni and Cu oxides and their mixtures were formed (particle diameters of 20 to 100 Å). Upon high-temperature heating, these nanoparticles were partially converted into CeO_2 and coarser mixed oxides of nickel with chromium, cerium with copper, and copper with chromium, as well as nickel and copper aluminates. In the course of reaction at 1173 K, Cu and Ni oxides were reduced with hydrogen to form Ni^0, Cu^0, and $NiCu_{3.8}$ (d = 2.08, 1.08, and 1.27 Å, respectively) as a loose polycrystalline film. On the

surface of the resulting α-Al_2O_3, semitransparent Ce_6O_{11} particles (50–60 Å) and coarser dense mixed phases were present. The catalyst retained its phase composition in the course of selective methane oxidation with the formation of synthesis gas.

The conversion of Ni and Cu aluminates into metal particles and the formation of $NiCu_{3.8}$ clusters under the action of H_2 and CH_4 were supported using TPR and electron microscopy with electron microdiffraction. The formation of a Ni–Cu alloy on Al_2O_3 in a reducing atmosphere upon the decomposition of CH_4 was also considered in a number of publications [34–38, 58]. It is likely that copper, which is reduced and oxidized more readily than nickel and other elements, plays a leading role in the reductive decomposition of $Ni(Cu)Al_2O_3$. Previously, we found that the promoting of the Co/Al_2O_3 catalyst with palladium prevented the formation of $CoAl_2O_4$ in both reducing (H_2, CO) and oxidizing atmospheres [59, 60]. As found by EXAFS, this was due to the formation of CoPd clusters and mixed oxides on the surface.

Optimum conditions for the selective oxidation of CH_4 on the reduced 9% NiCuCr/2% $Ce/(\theta + \alpha)$-Al_2O_3 catalyst in dilute mixtures with O_2 and Ar to form synthesis gas were determined: reaction temperature, 1173 K; $CH_4/O_2 = 2 : 1$; $\tau = 2.35–3.27$ ms; and $V = (1.17–1.53) \times 10^6$ h^{-1}. In this case, the conversion of methane was as high as 88–100% and the selectivity of CO and H_2 formation was 99.6–100 and 99.0–100%, respectively; CO_2 traces were also formed (0.005%).

The catalyst did not decrease its activity for 56 h; surface carbon deposition was not observed [61–63]. In terms of efficiency and output, the 9% NiCuCr/2% $Ce/(\theta + \alpha)$-Al_2O_3 catalyst was close to $NiCe/Al_2O_3$ [31], $LiNiLa/Al_2O_3$ [19], and Ni catalysts promoted with noble metals. Thus, further studies of the catalyst stability in the reaction of selective methane oxidation with the use of more concentrated mixtures of CH_4 with other alkanes are promising. Recent results [12, 20] suggest that, obviously, selective methane oxidation can be performed as an individual reaction using O_2 as an oxidizing agent or in combination with steam reforming on porous block supports of cordierite and metal alloys.

The selective oxidation of CH_4 on the 9% NiCuCr/2% $Ce/(\theta + \alpha)$-Al_2O_3 catalyst came into play in the first minutes (experiment times were 180 min) and occurred almost without the formation of CO_2; the residence time did not affect the composition of the resulting products. This suggests that the reaction occurred through the dissociative adsorption of CH_4 on Ni^0 and $NiCu_{3.8}$ clusters with the formation of carbon and atomic hydrogen, which dissolved in the $NiCu_{3.8}$ alloy. According to the results of TPO and TPD of oxygen, the activation of oxygen, which interacted with carbon, could occur at Cu^0, Ni^0, and $NiCu_{3.8}$ cluster particles. It is likely that the activation of individual components occurred at different cluster constituents: CH_4, at Ni atoms and O_2, at Cu atoms. Ce_6O_{11} can also be a source of active oxygen. Because copper was the predominant constituent of the catalyst, the rate of oxidation of carbon particles was higher than the rate of their formation; because of this, carbon was not accumulated (the balance on carbon was 100%).

The ability of the Ni–Cu–Cr catalyst to absorb the resulting atomic hydrogen in the bulk is of considerable importance for the mechanism of selective methane oxidation. It is well known that dissolved hydrogen was released from Ni, Fe, Co, and their alloys at surface sites where strongly bound hydrogen was chemisorbed. In the case of the Ni–Cu–Cr catalyst, this occurred at $T_{max} = 1123–1163$ K.

REFERENCES

1. Krylov, O.V., *Catal. Today*, 1993, vol. 18, p. 9.
2. Arutyunov, V.S. and Krylov, O.V., *Okislitel'nye prevrashcheniya metana* (Oxidative Conversions of Methane), Moscow: Nauka, 1998.
3. Prettre, M., Eichner, C.H., and Porrin, M., *Trans. Faraday Soc.,* 1946, vol. 43, p. 335.
4. Huft, M. and Schmidt, L.D., *J. Phys. Chem.*, 1993, vol. 97, p. 1815.
5. Hickman, F.A. and Schmidt, L.D., *J. Catal.*, 1992, vol. 138, p. 267.
6. Hickman, F.A., Haupfear, E.A., and Schmidt, L.D., *Catal. Lett.*, 1993, vol. 17, p. 223.
7. Lezaun, J., Gomes, J.P., Blanco, M.D., et al., *Stud. Surf. Sci. Catal.*, 1998, vol.119, p. 733.
8. Hofstad*, K. and Andersson, B., Stud. Surf. Sci. Catal.*, 1997, vol. 107, p. 429.
9. Schmidt, L.D. and Dietz, A., *Mater. Res. Soc. Symp. Proc.*, 1995, vol. 368, p. 299.
10. Safonov, M.S., Granovskii, M.S., and Pozharskii, S.B., *Zh. Fiz. Khim.*, 2000, vol. 74, p. 850 [*Russ. J. Phys. Chem.* (Engl. Transl.), vol. 74, p. 748].
11. RF Patent 2123 471, 1998.
12. Giroux, Th., Hwang, Sh., Lin, J., et al., *Appl. Catal., B*, 2005, vol. 56, p. 95.
13. Pavlova, S.N., Sadykov, V.A., Parmon, V.N., et al., *EuropaCat-5*, Limerick, Ireland, 2001, symp. 05, p. 3.
14. Pavlova, S.N. and Sadykov, V.A., *3rd World Congr. on Oxidation Catalysis*, 1997, part II, p. 567.
15. RF Patent 2144844, 2000.
16. Pavlova, S.N., Sazonova, N.N., Sadykov, V.A., et al., *Kinet. Katal.*, 2004, vol. 45, p. 622 [*Kinet. Catal.* (Engl. Transl.), vol. 45, p. 589].
17. Pavlova, S.N., Sazonova, N.N., Ivanova, J.A., et al., *Catal. Today*, 2004, vols. 91–92, p. 229.
18. Simakov, A.V. and Pavlova, S.N., *Chem. Sustainable Dev.*, 2003, vol. 11, p. 203.
19. Schicks, J., Neumann, D., Specht, U., et al., *EuropaCat-5*, Limerick, Ireland, 2001, symp. 01, p. 11.
20. Sadykov, V.A., Pavlova, S.N., Bunina, R.V., et al., *Kinet. Katal.,* 2005, vol. 46, p. 243 [*Kinet. Catal.* (Engl. Transl.), vol. 46, p. 227].

21. Tang, S., Lin, J., and Tan, K.Z., *Catal. Lett.*, 1998, vol. 51, p. 69.
22. Shen, S., Pan, L., Dong, Ch., et al., *Stud. Surf. Sci. Catal.*, 2001, vol. 136, p. 99.
23. Chi, W. and Jan, Q., *Stud. Surf. Sci. Catal.*, 1988, vol. 119, p. 849.
24. Liu, Sh. and Xiong, G., *Appl. Catal., A*, 2000, vol. 198, p. 261.
25. Choudhary, V.R., Mondal, K.C., and Mamman, A.S., *J. Catal.*, 2005, vol. 223, p. 36.
26. Guo, C., Zhang, J., Li, W., et al., *Catal. Today*, 2004, vol. 98, p. 36.
27. Lhu, W., Xiong, G., Han, W., and Jang, W., *Catal. Today*, 2004, vol. 95, p. 257.
28. Wang, H., Cong, J., and Jand, W., *Russia–China Seminar on Catalysis*, Novosibirsk, 2004, p. 43.
29. Claridge, J.B. and Jork, P.E., *J. Catal.*, 1998, vol. 180, p. 85.
30. Wang, J., Lin, Ch., Lhang, Y., et al., *Catal. Today*, 2004, vols. 91–92, p. 299.
31. Chu, W., Van, Q., Liu, Sh., and Xiong, G., *Stud. Surf. Sci. Catal.*, 2000, vol. 130, p. 3573.
32. Chen, H.-W., Wand, Ch.-Y., Yu, Ch.-H., et al., *Catal. Today,* 2004, vol. 97, p. 173.
33. Janlai, Ch., Shuben, L., Hua, G., and Zhengshi, Ch., *Acta Phys.-Chim. Sin.*, 1996, vol. 12, p. 429.
34. Reshetenko, T.V., Avdeeva, L.B., Ismagilov, Z.R., et al., *EuropaCat-5,* Limerick, Ireland, 2001, symp. 05, p. 149.
35. Reshetenko, T.V., Avdeeva, J.B., and Ismagilov, Z.R., *EuropaCat-5*, Limerick, Ireland, 2001, symp. 05, p. 1.
36. Molchanov, V.V. and Buyanov, R.A., *Kinet. Katal.*, 2001, vol. 42, p. 403 [*Kinet. Catal.* (Engl. Transl.), vol. 42, p. 366].
37. RF Patent 97103 664,1999.
38. Molchanov, V.V., Chesnokov, V.V., Buyanov, R.A., and Zaitseva, N.A., *Russia–China Seminar on Catalysis*, Novosibirsk, 2004, p. 54.
39. Sokol'skii, D.V., Golodova, L.S., Golodov, F.G., and Bolkhovitina, E.G., *Issledovanie katalizatorov gidrogenizatsii zhirov* (Fat Hydrogenation Catalysts), Alma-Ata: Akad. Nauk Kaz. SSR, 1958.
40. Wang, Q., Yao, J., Rong, J., et al., *Catal. Lett.,* 1990, vol. 4, p. 63.
41. Popova, N.M., Sokol'skii, D.V., and Popov, N.N., *Tezisy dokladov Vsesoyuznoi konf. "Kataliticheskie reaktsii v zhidkoi faze"* (Proc. All-Union Conf. on Liquid-Phase Catalytic Reactions), Alma-Ata, 1962, p. 31.
42. Popov, N.N., *Extended Abstracts of Cand. Sci. Dissertation*, Alma-Ata, 1964.
43. Altynbekova, K.A., *Extended Abstracts of Cand. Sci. Dissertation*, Alma-Ata, 1994.
44. Altynbekova, K.A., Popova, N.M., and Sokolova, L.A., *Seminar pamyati prof. V.V. Popovskogo "Zakonomernosti glubokogo okisleniya veshchestv na tverdykh katalizatorakh*" ("Deep Oxidations on Solid Catalysts," a Workshop in Memory of Prof. V.V. Popovskii), Novosibirsk, 2000, p. 242.
45. Popova, N.M., Babenkova, L.V., and Sokol'skii, D.V., *Izv. Akad. Nauk Kaz. SSR*, 1964, no. 2, p. 45.
46. Popova, N.M., *Vliyanie nositelya i struktury metallov na adsorbtsiyu gazov* (Effects of the Support and Metal Structure on Gas Adsorption), Alma-Ata: Nauka, 1980.
47. Popova, N.M., Salakhova, R.Kh., Dosumov, K., and Tungatarova, S.A., Affirmative Decision on Kazakh Pro-Patent no. 12-2/131, 2006.
48. Popova, N.M., Zheksenbaeva, Z.T., Kosmambetova, G.R., Sokolova, L.A., and Dosumov, K., *Zh. Fiz. Khim.,* 2001, vol. 75, p. 44 [*Russ. J. Phys. Chem.* (Engl. Transl.), vol. 75, p. 37].
49. Popova, N.M, Babenkova, L.V., and Savel'eva, G.A., *O sovremennom metode termodesorbtsii i ego ispol'zovanii v adsorbtsii i katalize* (Advanced Thermal Desorption Technique and Its Use in Adsorption and Catalysis), Alma-Ata: Inst. Organicheskogo Kataliza i Elektrokhimii, 1985.
50. Grigor'eva, V.P., Popova, N.M., Zheksenbaeva, Z.T., Sass, A.S., Salakhova, R.Kh., and Dosumov, K.D., *Izv. MON RK, Ser. Khim.*, 2002, no. 5, p. 63.
51. Komashko, L.V., Zheksenbaeva, Z.T., Popova, N.M., and Dosumov, K., *Izv. Min. Obr. Nauki Resp. Kaz., Nats. Akad. Nauk Resp. Kaz., Ser. Khim.*, 2002, no. 6, p. 68.
52. Popova, N.M., Zheksenbaeva, Z.T., Dosumov, K., Sass, A.S., and Salakhova, R.Kh., *Izv. Min. Obr. Nauki Resp. Kaz., Nats. Akad. Nauk Resp. Kaz., Ser. Khim.*, 2003, no. 5, p. 50.
53. Korzhenevskaya, T.N., Zubritskaya, N.T., and Kozlova, O.V., *Zh. Prikl. Khim.,* 1997, vol. 70, p. 1665 [*Russ. J. Appl. Chem.* (Engl. Transl.), vol. 70, p. 1582].
54. Munteanu, G., Ilieva, Z., Tabakova, T., and Andreeva, D., *Heterogeneous Catalysis: Proc. 9th Int. Symp.*, Varna, 2000, p. 435.
55. Zheksenbaeva, Z.T., *Extended Abstracts of Cand. Sci. Dissertation*, Almaty, 2005.
56. *Hydrogen in Metals*, Alefeld, G. and Volkl, J., Eds., Berlin: Springer, 1978, vol. 1.
57. Popova, N.M., Babenkova, L.V., and Savel'eva, G.A., *Adsorbtsiya i vzaimodeistvie prosteishikh gazov s metallami VIII gruppy* (Adsorption and Interaction of the Simplest Gases with Group VIII Metals), Alma-Ata: Nauka, 1979.
58. Avdeeva, L.B., Goncharova, O.V., Kochubey, D.J., et al., *Appl. Catal., A*, 1996, vol. 141, p. 117.
59. Popova, N.M. and Savel'eva, G.A., *Teor. Eksp. Khim.*, 1991, no. 6, p. 646.
60. L'dokova, G.M., Popova, N.M., Sass, A.S., et al., *Proc. Conf. "Catalysis in the Eve of the XXI Century: Science and Engineering,"* Novosibirsk, 1997.
61. Popova, N.M., Zheksenbaeva, Z.T., Sass, A.S., Dosumov, K., and Salakhova, R.Kh., *Izv. Min. Obr. Nauki Resp. Kaz., Nats. Akad. Nauk Resp. Kaz., Ser. Khim.*, 2003, no. 5, p. 50.
62. Dosumov, K., Tungatarova, S.A., Popova, N.M., and Salakhova, R.Kh., *7th Int. Conf. on Nanostructured Materials,* Wiesbaden, 2004, p. 31.
63. Dosumov, K., Salakhova, R.Kh., Popova, N.M., Tungatarova, S.A., Grigorieva, V.P., Komashko, L.V., and Sass, A.S., *J. Alloys Compd.*, 2007, vols. 434–435, p. 796.